

# Critical synchronization dynamics of the Kuramoto model on connectome and small world graphs

Géza Ódor MFA Complex Systems, Budapest

Jeffrey Kelling HZDR Dresden, Róbert Juhász, Wigner FK Budapest

Theoretical research and experiments suggest that the brain operates at or near a **critical state** between sustained activity and an inactive phase, exhibiting optimal computational properties (see: *Beggs & Plenz J. Neurosci. 2003; Chialvo Nat. Phys. 2010; Haimovici et al. PRL 2013* )

Individual neurons emit periodic signals  
(*Y. Penn et al PNAS 113 (2016) 3341*)

→ Criticality at the **synchronization transition critical point**

# Why would be brain near criticality ?

## Pros:

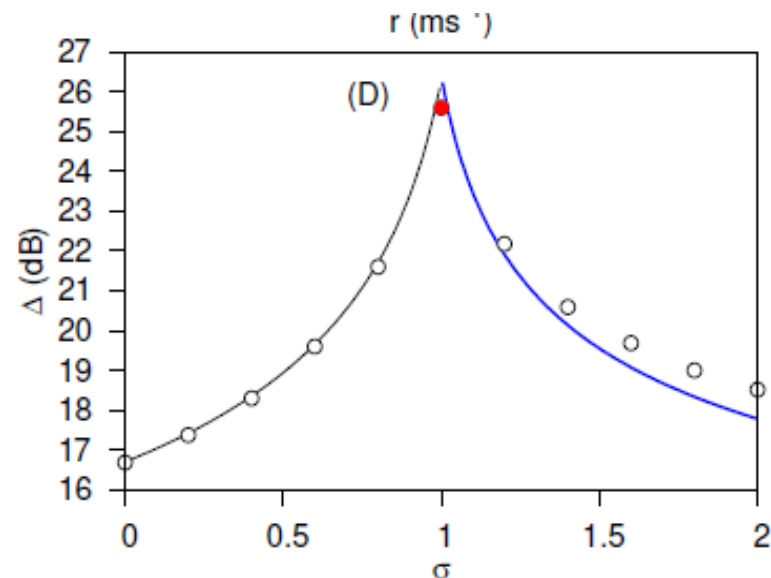
Diverging fluctuations →  
High sensitivity to stimuli

Diverging correlation functions →  
Optimal transmission and  
storage of information

Maximal information processing and computational performance

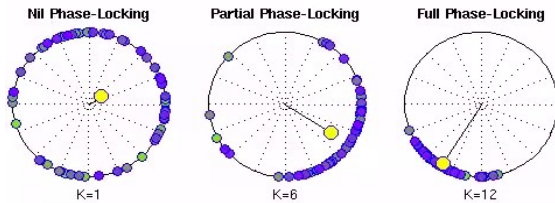
**Cons:** Tuning to critical point

Self-organized critical mechanism ?



# Kuramoto oscillator model (1975)

## Kuramoto Oscillators



Nil, partial and full phase-locking in an all-to-all network of Kuramoto oscillators. Phase-locking is governed by the coupling strength  $K$  and the distribution of intrinsic frequencies  $\omega$ . Here, the intrinsic frequencies were drawn from a normal distribution ( $M=0.5\text{Hz}$ ,  $SD=0.5\text{Hz}$ ). The yellow disk marks the phase centroid. Its radius is a measure of coherence.

$$\dot{\theta}_i(t) = \omega_{i,0} + K \sum_j W_{ij} \sin[\theta_j(t) - \theta_i(t)]$$

phases  $\theta_i(t)$

global coupling  $K$  is the control parameter

weighted adjacency matrix  $W_{ij}$

$\omega_{i,0}$  is the intrinsic frequency of the  $i$ -th oscillator,

Order parameter : average phase:

$$R(t) = \frac{1}{N} \left| \sum_{j=1}^N e^{i\theta_j(t)} \right|$$

$R(t \rightarrow \infty) > 0$  for  $K > K_c$ ,  $R(t \rightarrow \infty) = 0$  for  $K \leq K_c$  as  $R \propto (1/N)^{1/2}$

Exhibits an initial growth:  $R(t, N) = N^{-1/2} t^\eta f_\uparrow(t/N^2)$  for incoherent initial state

Critical synchronization transition for  $D > 4$  spatial dimensions, which is mean-field like: i.e.  $D \rightarrow \infty$  (full graph)

The dynamical behavior suffers very strong corrections to scaling and *chaoticity*, see:

Róbert Juhász, Jeffrey Kelling and Géza Ódor:

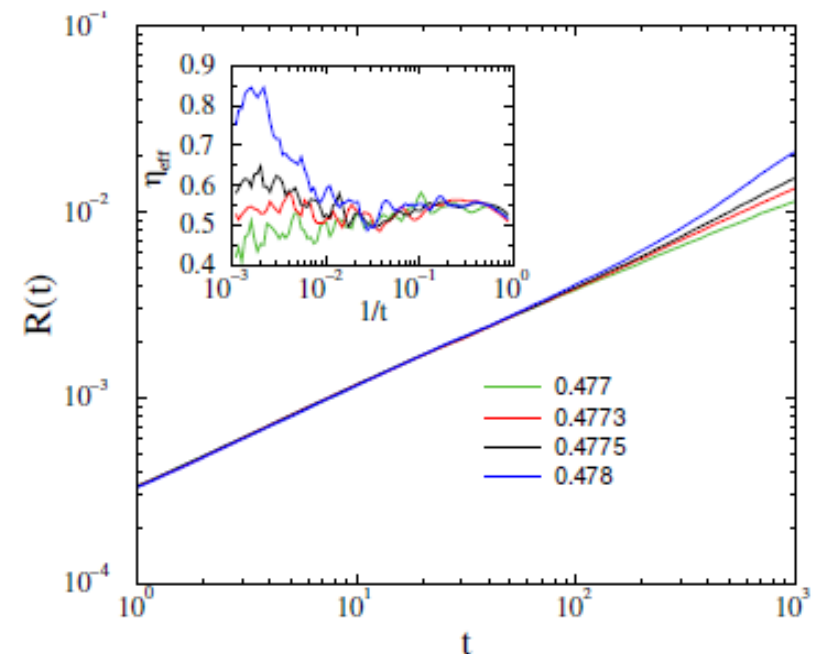
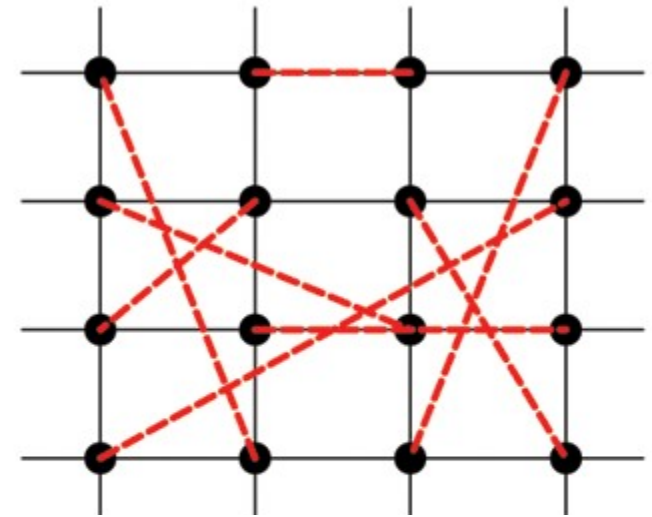
Critical dynamics of the Kuramoto model on sparse random networks

J. Stat. Mech. (2019) 053403

# Growth of synchronization on sparse, synthetic small-world networks

2D lattices of linear size  $L = 6000$ ,  
periodic boundary conditions,  
+ extra random long link between  
connecting any edges:  $\langle k \rangle = 5$ ,  
*90.000.000 edges*

Growth runs from random initial state  
Runge-Kutta-4 parallelized for GPUs  
Maximum time:  $t_{max} = 1000$ ,  
average over: *10000* independent  $\omega_i$   
realizations  
Critical point located at  $K=0.4773$   
Critical exponent:  $\eta = 0.55 (10)$



# Determination of the characteristic time exponent $\tau_t$

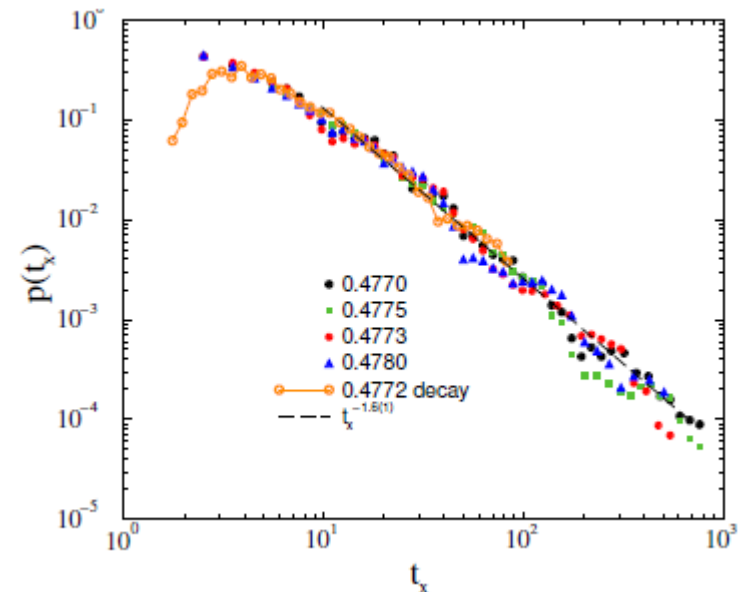
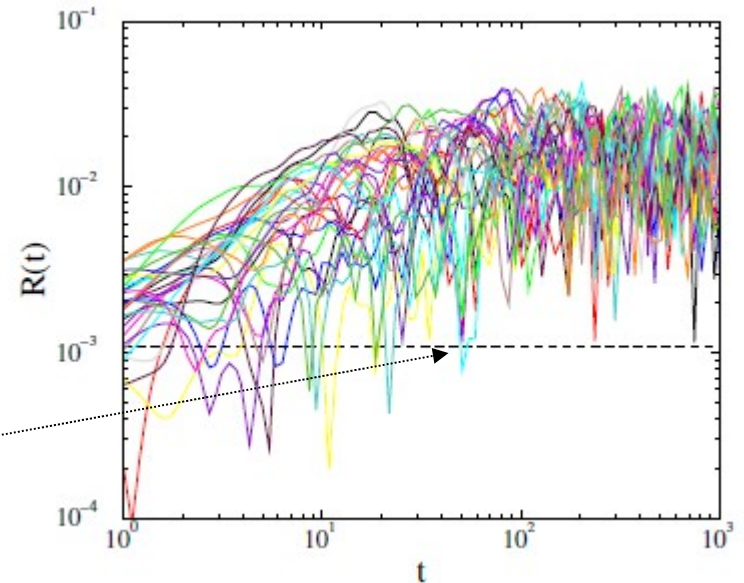
Measure characteristic times  $t_x$  of first dip below:  $R_c = (1/N)^{1/2}$

average over: 10.000 independent  $\omega_i$  distribution realizations

Histogramming of  $t_x$  at the critical point

Critical exponent:  $\tau_t = 1.6 (1)$  obtained by fitting for the PL tails

First estimate for  $\tau_t$  in mean-field

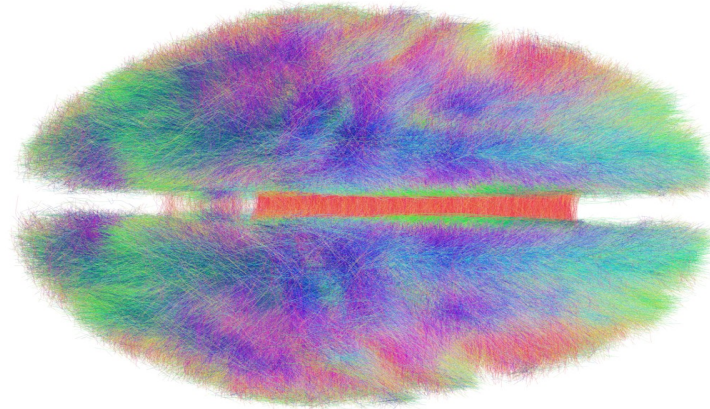


# What do we know about neuron networks ?

The largest precisely explored structural networks contains  
~302 neurons (C. Elegans) (very recently fruit fly map is reported)



Connectomes, obtained by approximative methods like diffusion MRI  
contain  $< 10^6$  nodes (voxels)



Recently DMRI tractography was confirmed by tract-tracing in ferret

# Open Connectome Large Human graphs

Diffusion and structural MRI images with

$1 \text{ mm}^3$  voxel resolution :

$10^5 - 10^6$  nodes

Hierarchical modular graphs

Top level: 70 brain region (Desikan atlas)

Lower levels: Deterministic tractography:

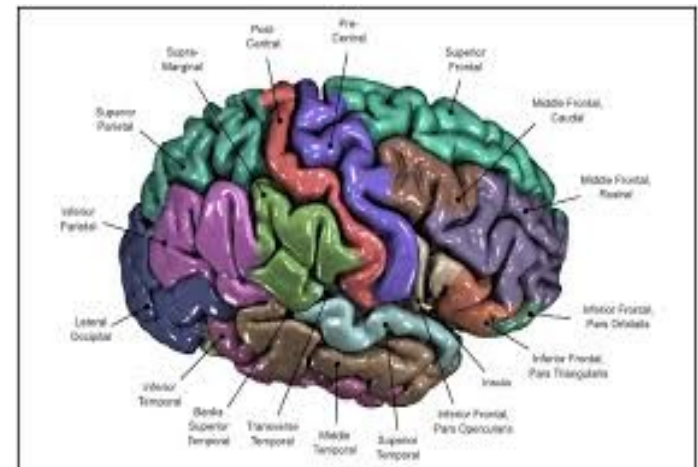
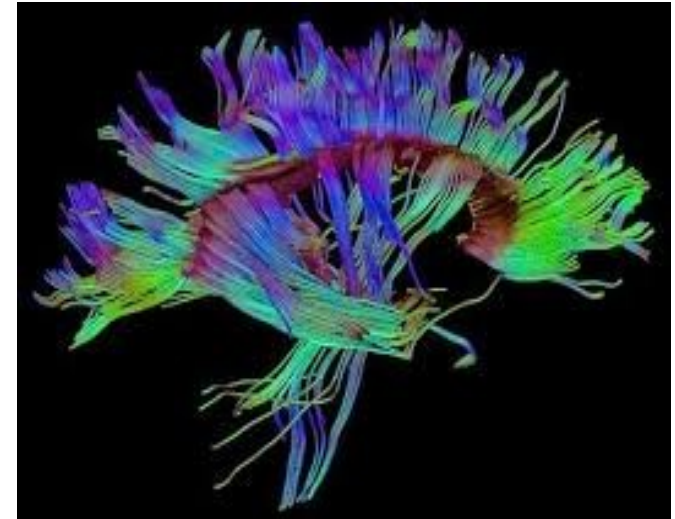
Fiber Assignment by Continuous Tracking  
(FACT) algorithm

Map : voxel  $\rightarrow$  vertex ( $\sim 10^7$ )

fiber  $\rightarrow$  edge ( $\sim 10^{10}$ )

+ noise reduction  $\rightarrow$  graph

undirected, weighted



OPEN

## The topology of large Open Connectome networks for the human brain

Received: 18 December 2015

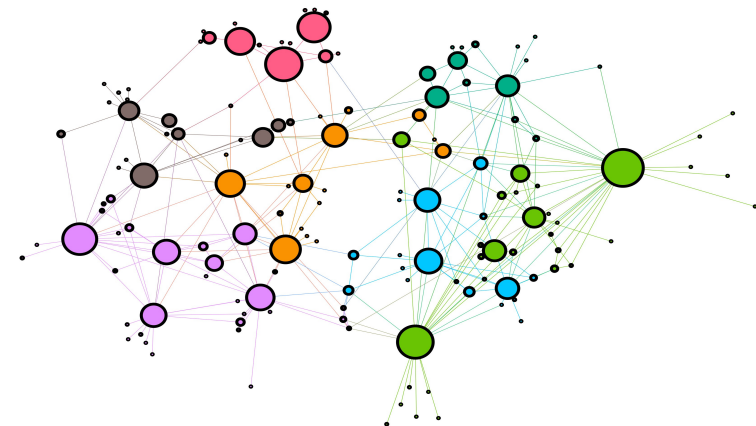
Accepted: 12 May 2016

Published: 07 June 2016

Michael T. Gastner<sup>1,2</sup> & Géza Ódor<sup>2</sup>

The structural human connectome (i.e. the network of fiber connections in the brain) can be analyzed at ever finer spatial resolution thanks to advances in neuroimaging. Here we analyze several large data sets for the human brain network made available by the Open Connectome Project. We apply statistical model selection to characterize the degree distributions of graphs containing up to  $\simeq 10^6$  nodes and  $\simeq 10^8$  edges. A three-parameter generalized Weibull (also known as a stretched exponential) distribution is a good fit to most of the observed degree distributions. For almost all networks, simple power laws cannot fit the data, but in some cases there is statistical support for power laws with an exponential cutoff. We also calculate the topological (graph) dimension  $D$  and the small-world coefficient  $\sigma$  of these networks. While  $\sigma$  suggests a small-world topology, we found that  $D < 4$  showing that long-distance connections provide only a small correction to the topology of the embedding three-dimensional space.

Small world, still finite dimensional,  
non-scale free,  
universal modular graphs



# Kuramoto solution for the KKI-18 graph with $N= 836\ 733$ nodes and $41\ 523\ 931$ weighted edges

The synchronization transition point

determined by growth as before

KKI-18 has  $D = 3.05 < 4 \rightarrow$

No real phase transition, crossover

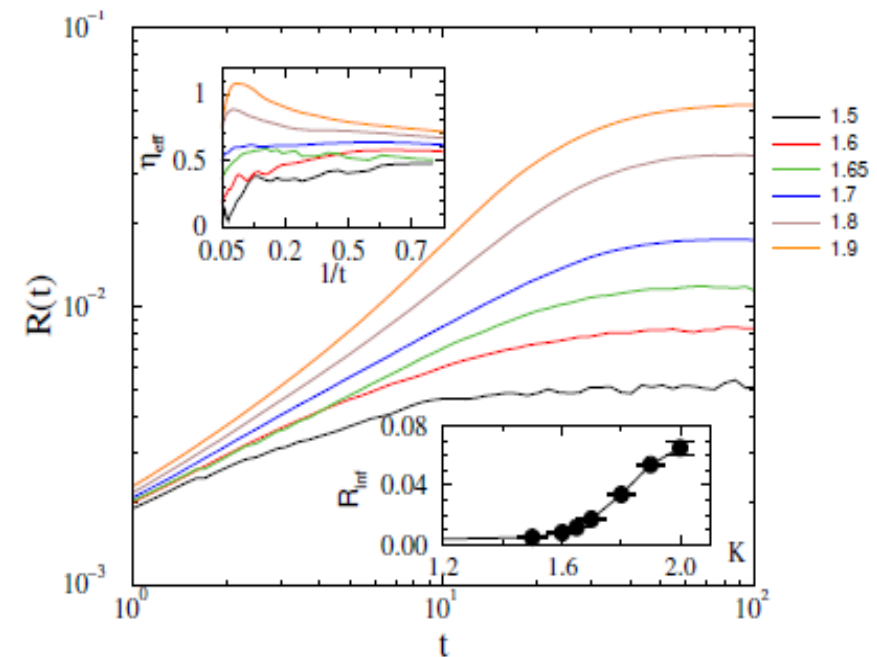
Due to the fat-tailed link weight

distribution, incoming weight

normalization is applied:

$$W'_{i,j} = W_{i,j} / \sum_{j \in \text{neighb. of } i} W_{i,j}$$

$K_c = 1.7$  and growth exponent:  $\eta = 0.6(1)$



# Duration distribution for the KKI-18 graph

Measure characteristic times  $t_x$  of first

dip below:  $R_c = (1/N)^{1/2}$

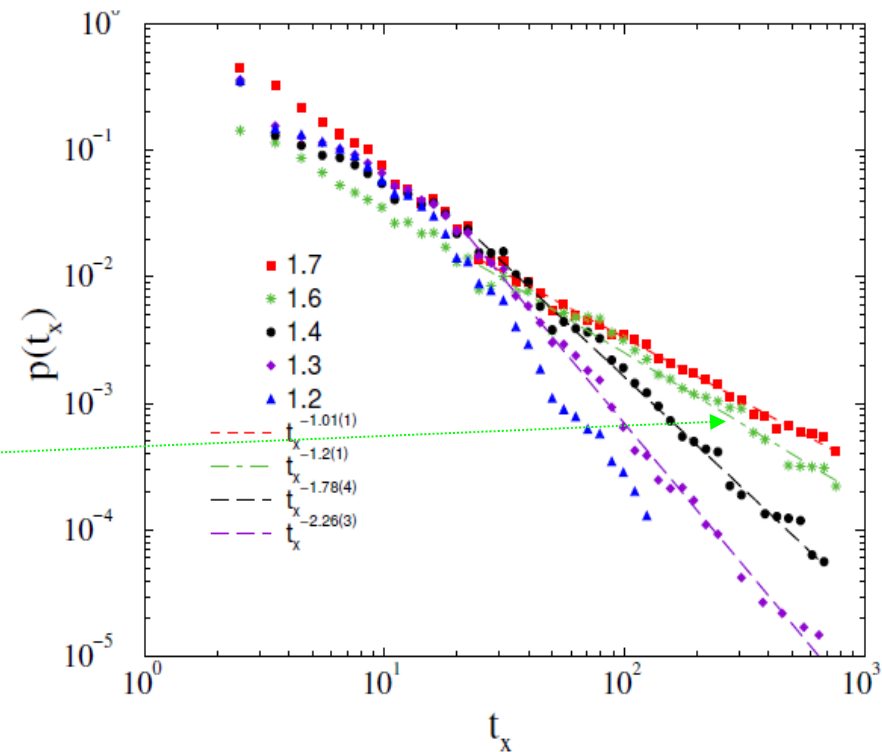
average over: 10.000 independent  $\omega_i$   
realizations

Histogramming of  $t_x$  at the critical point

Critical exponent:  $\tau_t = 1.2 (1)$

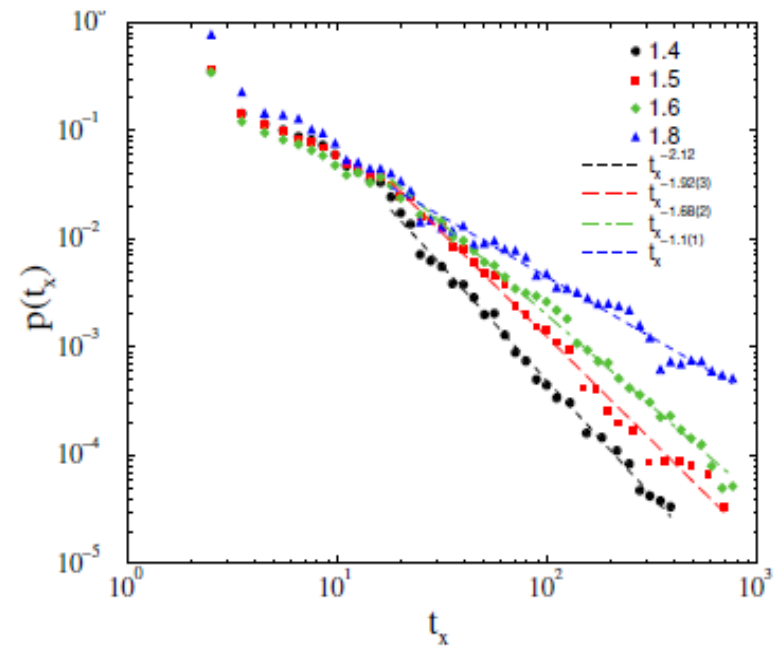
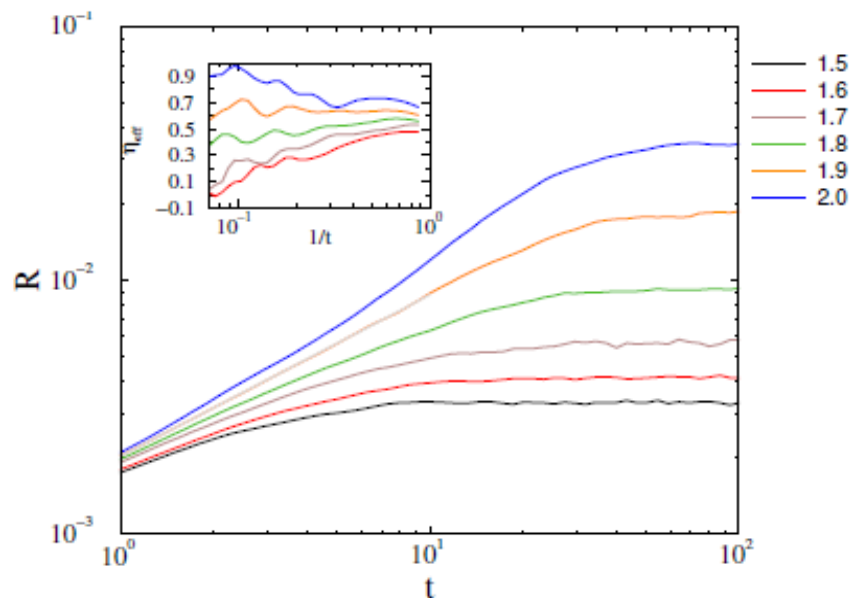
obtained by fitting for the PL tails

Below the transition point :  $K < 1.6$   
non-universal power laws in the range  
of experiments of activity durations :  
 $1.5 < \tau_t < 2.4$  (*Palva et al 2013*)



# Inhibitory (negative) links

Inhibitions: 20% of **links**:  $w_{ij} \rightarrow -w_{ij}$  randomly



$K_c$  increases to  $1.9(1)$ , but  $\eta = 0.6(1)$  remains the same, and below it:

**Duration scaling exponent within experimental range:  $1.5 < \tau_t < 2.4$**   
*J.M. Palva et al PNAS 110 (2013) 3585*

# Inhibitory nodes

Inhibitions: 5% of **nodes**:  $w_{ii} \rightarrow -w_{ii}$  randomly

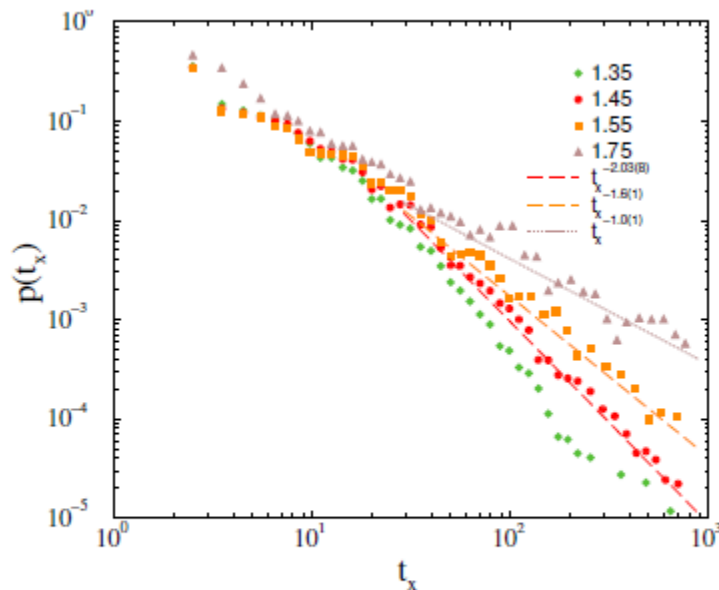


**Figure 9.** Duration distribution of  $t_x$  on the *KKI-18-I* model in case of 5% inhibitory node assumption for  $K = 1.35$  (+),  $K = 1.45$  (bullets), 1.55 (boxes), 1.75 (triangles). The dashed line shows PL fits to the tail region:  $t_x > 20$ .

$K_c = 1.7(1)$  and  $\eta = 0.6(1)$  remains the same. Sub-critically:

**Duration scaling exponent within experimental range:  $1.5 < \tau_t < 2.4$**   
*J.M. Palva et al PNAS 110 (2013) 3585*

# Galilean invariance of the Kuramoto model with respect to the $\omega_i$ distribution

Brain experiments:  $\omega_i > 0$

distributions are narrow:  $\sigma_i \sim 0.02$

and have mean value:  $\langle \omega_i \rangle \sim 0.05$

$$\dot{\theta}_i(t) = \omega_{i,0} + K \sum_j W_{ij} \sin[\theta_j(t) - \theta_i(t)]$$

$\langle \omega_i \rangle \neq 0$  can be gauged out by a rotating coordinate system

Rescaling of  $\omega_i$  as :  $\omega_i \rightarrow a\omega_i'$     $t \rightarrow (1/a)t'$     $K \rightarrow aK'$

**Existing results can be transformed for later times and weaker couplings**

# Conclusions

Heterogeneity effects are considered on large connectomes and random small-world graphs

This enables us to distinguish from finite size rounding effects

Large OCP graphs show: ~ degree distribution universality, finite Dimensionality and small-worldness

For Erdős-Rényi : Mean-field dynamical scaling with ugly corrections  
New method to determine crossover to synchronization and  $\tau_t$

Below the transition point non-universal scaling of phase synchronization  
“Frustrated synchronization” ~ Griffiths Phase ?

Durations, with exponents agreeing in vivo activity experiments for humans

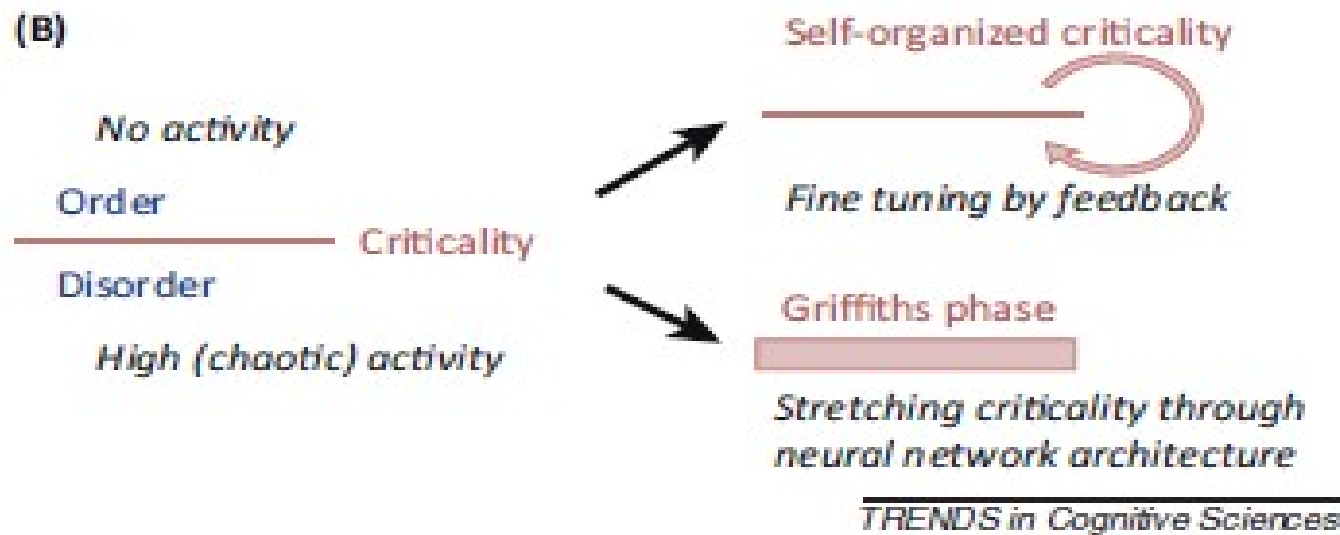
Effects of inhibitory links, nodes

Invariance with respect to frequency distributions

Insensitivity for additive Gaussian noise

*G.Ó and J. K, arXiv:1903.00385, accepted in Scientific Reports*

# Explanations for tuning to criticality



SOC  $\leftrightarrow$  GP do not exclude each other

For SOC we need a responsible feedback mechanism,

GP can occur spontaneously in heterogeneous systems

GP ~ Frustrated synchronization

# OPEN CONNECTOME PROJECT

COLLECTIVELY REVERSE-ENGINEERING THE BRAIN ONE SYNAPSE AT A TIME.

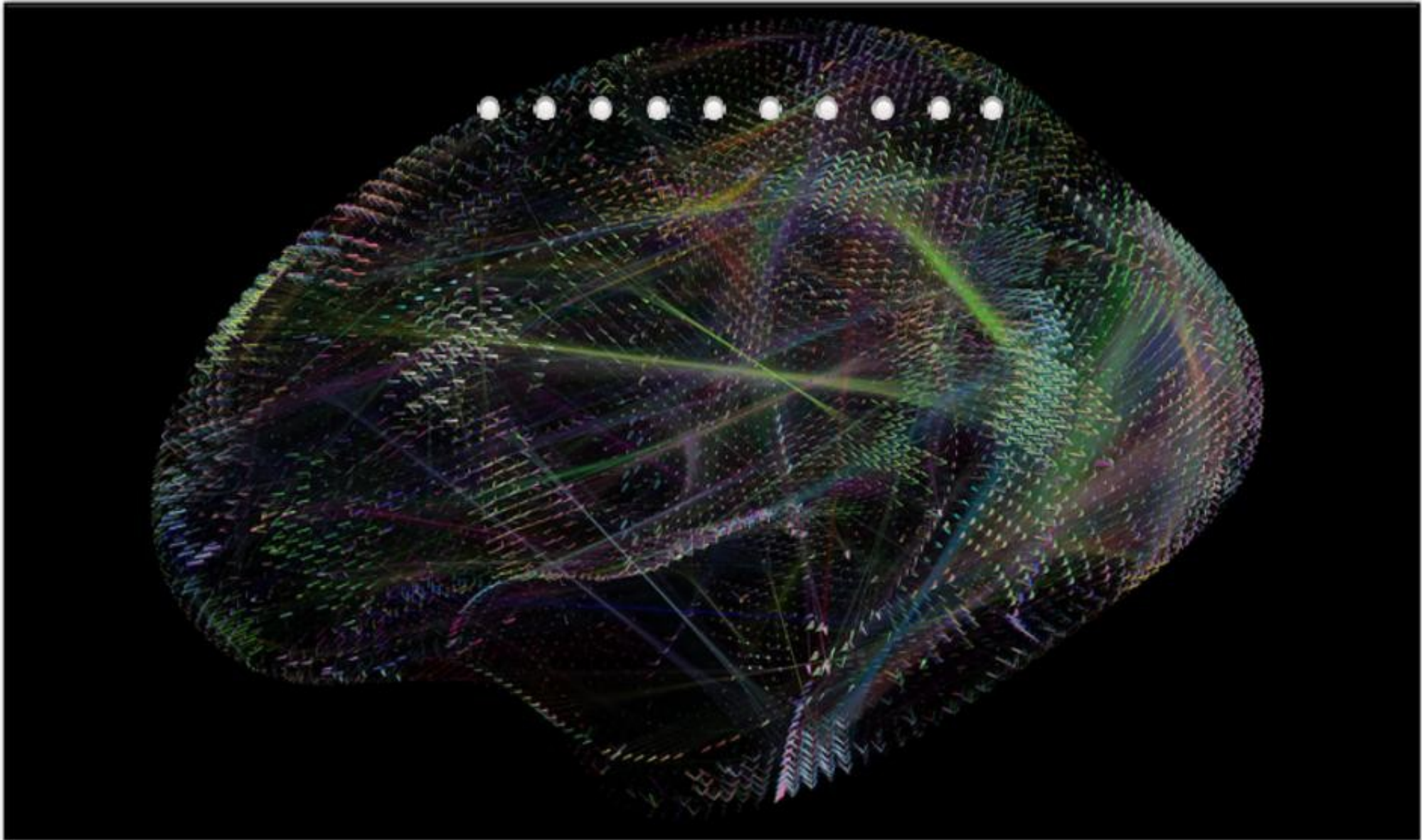
connectHOME

INFO

IMAGES

GRAPHS

HELP

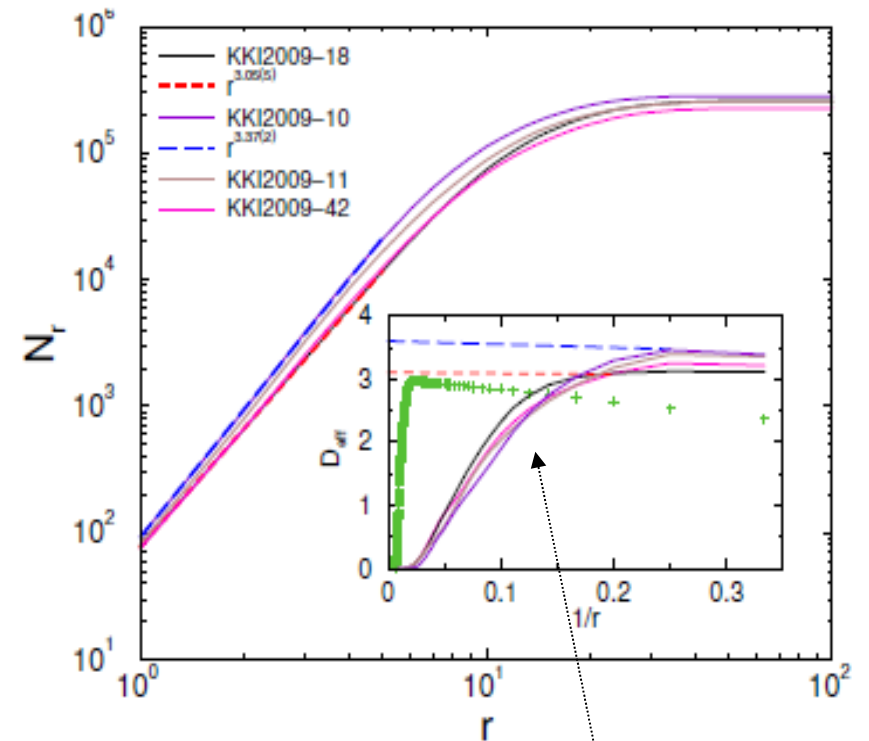


Freely downloadable images and graphs of humans and animals:  
<https://neurodata.io>.

# OCP graph dimension measurements

Breadth-first search algorithm from each vertex

$$D < 4$$



$$N_r \sim r^D$$

$$D_{eff} = d \ln(N_r) / d \ln r$$

# OCP graph analysis

Degree distribution : scale-free ?

Maximum likelihood method

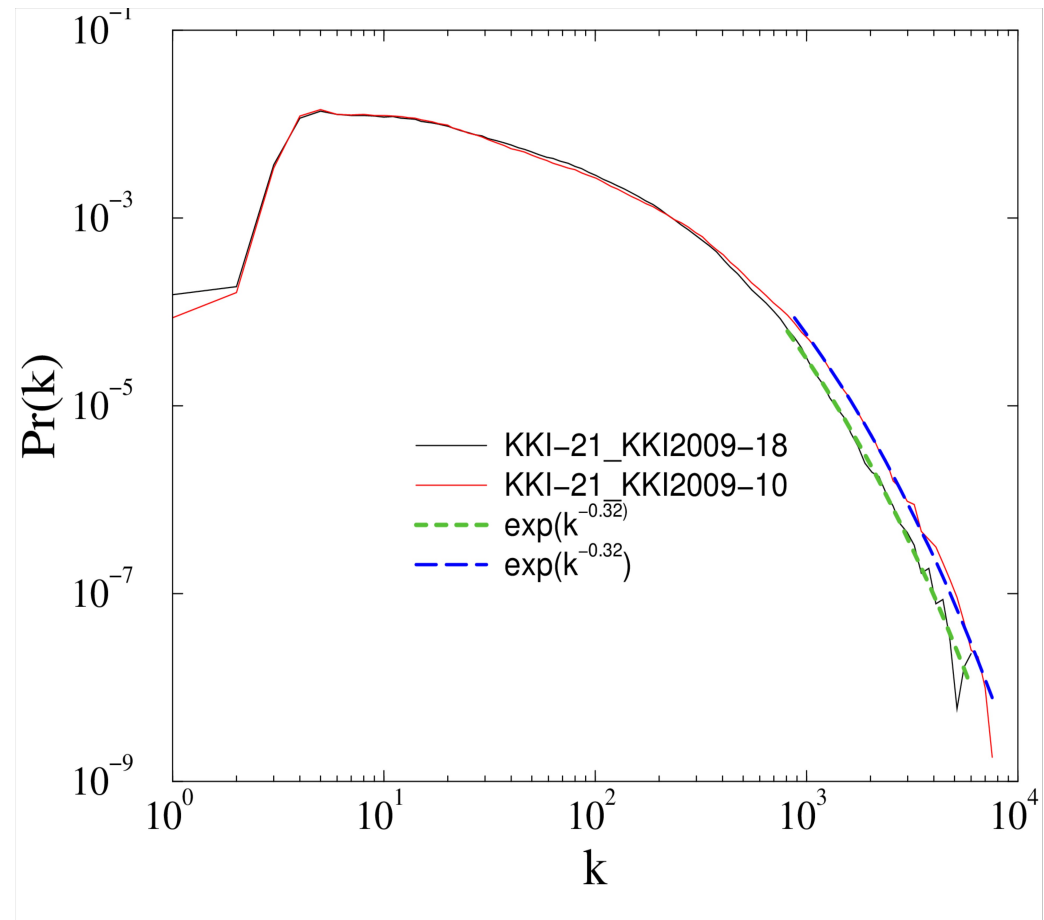
$$\mathcal{L}(\mathbf{v}) = \prod_{i=1}^N \Pr(k_i, \mathbf{v}).$$

Akaike information theory model selection:

$$AIC_c = -2\ln(\mathcal{L}(\hat{\mathbf{v}})) + 2K + \frac{2K(K+1)}{N-K-1}$$

$v_1, v_2, \dots, v_K$  parameters,  
maximizing  $\mathcal{L}$

Best model : **stretched exponential,**  
**with ~ universal exponent**



# Kuramoto model on the random Erdős-Rényi graph, desynchronization

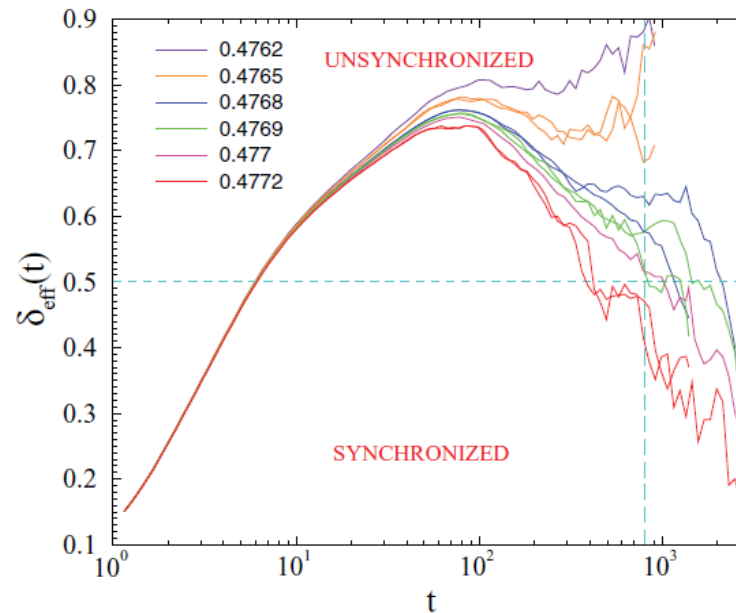
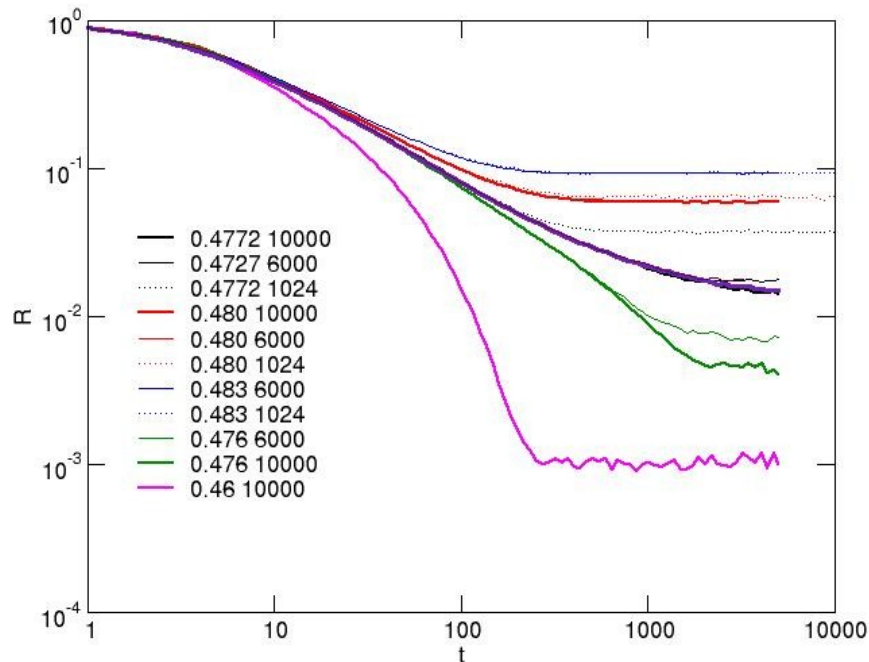


**Figure 7.** Effective decay exponents  $\delta_{\text{eff}}(t)$  as a function of time obtained numerically in the ER graph ( $k=1$ ) combined with a 2d lattice, for different values of  $K$  and sizes  $N=6000$  (thin lines) and  $N=10000$  (thick lines). The dashed horizontal line indicates the asymptotic value  $\delta=1/2$  of the mean-field universality class, while the vertical line shows the estimated cutoff time for the larger size.

Runge-Kutta-4 GPU solution for zero centered  $\omega_i$  of unit variance

Decay of  $R(t)$  near the critical point for different sizes

Mean-field behavior + non-monotonic corrections to scaling (?)

# OCP small world coefficient

$$\sigma = \frac{C/C_r}{L/L_r}$$

$$C^\Delta = \frac{\text{number of closed triplets}}{\text{number of connected triplets}}$$

$$L = \frac{1}{N(N-1)} \sum_{j \neq i} d(i, j), \quad L_r = \frac{\ln(N_l) - 0.5772}{\ln \langle k \rangle} + 1/2$$

KKI	$N$	$N_{\text{edges}}$	$\langle k \rangle$	$L$	$L_r$	$C^W$	$C^\Delta$	$C_r$	$\sigma^W$	$\sigma^\Delta$
10	$9.40 \times 10^5$	$8.68 \times 10^7$	184.71	11.38	3.02	$5.94 \times 10^{-1}$	$3.20 \times 10^{-1}$	$1.97 \times 10^{-4}$	803.26	433.09
11	$8.63 \times 10^5$	$7.07 \times 10^7$	163.84	12.25	3.07	$5.99 \times 10^{-1}$	$3.24 \times 10^{-1}$	$1.90 \times 10^{-4}$	789.23	427.69
12	$7.44 \times 10^5$	$4.98 \times 10^7$	133.79	13.91	3.14	$6.02 \times 10^{-1}$	$3.58 \times 10^{-1}$	$1.80 \times 10^{-4}$	757.12	450.43
13	$8.46 \times 10^5$	$5.93 \times 10^7$	140.17	12.96	3.14	$6.02 \times 10^{-1}$	$3.56 \times 10^{-1}$	$1.66 \times 10^{-4}$	881.74	521.58
14	$7.70 \times 10^5$	$5.36 \times 10^7$	139.10	13.10	3.13	$6.01 \times 10^{-1}$	$3.62 \times 10^{-1}$	$1.81 \times 10^{-4}$	794.64	478.99
15	$8.47 \times 10^5$	$6.94 \times 10^7$	163.84	12.80	3.06	$5.99 \times 10^{-1}$	$3.32 \times 10^{-1}$	$1.94 \times 10^{-4}$	740.79	411.13
16	$7.60 \times 10^5$	$5.70 \times 10^7$	150.11	12.03	3.09	$6.02 \times 10^{-1}$	$3.38 \times 10^{-1}$	$1.98 \times 10^{-4}$	782.48	438.63
17	$7.87 \times 10^5$	$5.20 \times 10^7$	132.29	13.00	3.16	$6.02 \times 10^{-1}$	$3.73 \times 10^{-1}$	$1.68 \times 10^{-4}$	869.74	529.15
18	$8.49 \times 10^5$	$6.63 \times 10^7$	156.21	11.30	3.09	$5.98 \times 10^{-1}$	$3.58 \times 10^{-1}$	$1.84 \times 10^{-4}$	888.09	531.35
19	$7.31 \times 10^5$	$4.94 \times 10^7$	134.99	13.17	3.14	$6.02 \times 10^{-1}$	$3.59 \times 10^{-1}$	$1.85 \times 10^{-4}$	775.96	462.90

**Table 4.** Summary of small-world properties for the studied KKI graphs.  $N, N_{\text{edges}}$ : number of nodes and edges.  $\langle k \rangle$ : mean degree.  $L$ : average shortest path length.  $L_r$ : expectation value for the average shortest path length in Erdős-Rényi graphs with the same  $N$  and  $N_{\text{edges}}$ .  $C^W, C^\Delta$ : clustering coefficients defined by Eq. 10 and 11, respectively.  $C_r$ : mean clustering coefficient in Erdős-Rényi graphs.  $\sigma^W, \sigma^\Delta$ : small-world coefficient defined by Eq. 9, based on either  $C^W$  or  $C^\Delta$ .

Finite graph dimension  $\leftrightarrow$  small world network ( $\sigma > 1$ )

# The effect of additive stochastic noise

Gaussian distributed annealed noise is added:

$$\dot{\theta}_i(t) = \omega_{i,0} + K \sum_j W_{ij} \sin[\theta_j(t) - \theta_i(t)] + s\xi(i)$$

Negligible effect:

